Light-Activated, Multi-Semiconductor Hybrid Microswimmers

Étude O'Neel-Judy, Dylan Nicholls, John Castañeda, and John G. Gibbs*

Using a dynamic fabrication process, hybrid, photoactivated microswimmers made from two different semiconductors, titanium dioxide (TiO_2) and cuprous oxide (Cu_2O) are developed, where each material occupies a distinct portion of the multiconstituent particles. Structured light-activated microswimmers made from only TiO_2 or Cu_2O are observed to be driven in hydrogen peroxide and water most vigorously under UV or blue light, respectively, whereas hybrid structures made from both of these materials exhibit wavelength-dependent modes of motion due to the disparate responses of each photocatalyst. It is also found that the hybrid particles are activated in water alone, a behavior which is not observed in those made from a single semiconductor, and thus, the system may open up a new class of fuel-free photoactive colloids that take advantage of semiconductor heterojunctions. The TiO_2/Cu_2O hybrid microswimmer presented here is but an example of a broader method for inducing different modes of motion in a single light-activated particle, which is not limited to the specific geometries and materials presented in this study.

Active microswimmers[1–6] are particles that are propelled autonomously in a fluid. These systems are not only interesting from a fundamental point-of-view, as many have led to novel physical phenomena[7–9] including motility-induced phase separation[10] and other collective behavior,[11–14] but several practical applications have also been presented ranging from environmental remediation[15,16] to medicine,[17,18] to name only a couple. However, much work remains to be done in order for the field to progress toward the realization of the most exciting and promising applications, starting with the establishment of the next generation of advanced active microswimmer systems. In this study, we develop and explore multi-semiconductor, light-activated hybrid microswimmers that exhibit wavelength-dependent modes of motion, which we expect will open new avenues in performing complex tasks at small scales.

One of the most prevalent means for achieving autonomous motion at the microscale exploits a catalyzed chemical reaction occurring on a particle's surface.[19–22] In such systems, the

location of the reaction site, i.e., where the catalyst is positioned on the particle, along with particle shape, have been shown to be the dominant factors determining the kinds of motion exhibited.[11,23–25] Thus, by targeted design, it is possible to tune the modes of active motion by systematically altering these parameters. With this in mind, it would be reasonable to imagine that fabricating a microswimmer with multiple catalysts could be a viable approach for achieving different modes of motion in the same particle. Although micro- and nanoswimmers[26] with more than one catalyst are fairly common in the literature, the motion is typically of one variety. For example, bimetallic cylindrical nanomotors made from gold and platinum move translationally toward the platinum site in hydrogen peroxide and water.[27,28] In such systems, the speed can be altered by changing the concentration of the chemical fuel, but the mode of motion, i.e., translational motion toward the platinum site, stays the same. This is likely due to the ratio relating the catalysts' turnover rates remaining constant despite modulation of the fuel concentration. In order to activate multiple modes of motion, one possible route could entail developing a system in which this ratio is not constant but depends upon environmental factors. This route has yet to be explored to the best of our knowledge; one of the closest studies investigated a mixed population of otherwise identical light-activated swimmers loaded with various dyes.[29] The authors showed such particles can be actuated independently from others loaded with a dissimilar dye, but nevertheless the swimmers show only one mode of motion. In contrast, here we designed a hybrid microswimmer from two photocatalytic semiconductors that decompose hydrogen peroxide at different rates depending upon the color of the activating light source, and consequently, the particles exhibit wavelength-dependent motive behavior.

We realized such a system by employing a dynamic fabrication method that enables developing particles with complex geometries from a wide range of materials and material combinations.[30–32] We used this technique recently to investigate the dynamics of structured photoactive particles where a large portion of the structural underpinning consisted of a photocatalyst, titanium dioxide (TiO_2), and we found such particles exhibit motion that is sensitively shape-dependent.[33] Microswimmers made from photoactivated semiconductors[34–44] have several advantages in comparison to those made from

É. O'Neel-Judy, Dr. D. Nicholls, J. Castañeda, Prof. J. G. Gibbs
Department of Physics and Astronomy
Northern Arizona University
Flagstaff, AZ 86011, USA
E-mail: john.gibbs@nau.edu

The ORCID identification number(s) for the author(s) of this article can be found under https://doi.org/10.1002/smll.201801860.

1801860 (1 of 6)

traditional metal catalysts like platinum, which include significantly lower cost, resistance to catalyst poisoning, the activity can be easily switched on-and-off, and the turnover rate is a function of both light intensity and wavelength. This latter property is key to our study here as disparity in the activities of the individual catalysts making up the hybrid structures is critical for achieving wavelength-dependent modes of motion. In particular, we focus upon photoactive hybrid microswimmers fabricated from both TiO_2 and copper (I) oxide (Cu_2O), which are active over different ranges of wavelength, but we note many other materials and material combinations could be realized using the same method.

We investigated the dynamics of particles made only from TiO_2 or Cu_2O (see **Figure 1**a,b) as control experiments in addition to the hybrid microswimmer constructed from both of these materials (Figure 1c). The controls were fabricated by depositing a thick layer ($\approx$1–3 µm) of either the semiconductor TiO_2 or the pure metal Cu by electron-beam evaporation at an oblique angle of $\approx$85°. TiO_2 was evaporated as an oxide, and was subsequently annealed at 500 °C for 2 h to obtain primarily the more photoactive anatase phase, while Cu was converted to Cu_2O after deposition by annealing in oxygen at 100 °C for 30 min: $4Cu + O_2 \rightarrow 2Cu_2O$.[45] To ensure uniformity between the structures, a close-packed monolayer of monodisperse silica (SiO_2)

microspheres (either 2 or 3 µm in diameter) served as nucleation centers for the depositing material,[33,46] which ultimately formed elongated "arms" (see Figure 1a,b). In order to develop the TiO_2/Cu_2O hybrid microswimmers shown in Figure 1c, we initially deposited TiO_2 at an oblique angle onto spherical microparticles, identical to the process depicted in Figure 1a. Temperatures high enough to obtain the anatase phase of TiO_2 would convert Cu to CuO as opposed to the desired oxide Cu_2O, and so before depositing the Cu arm, the sample was removed from the chamber and annealed at 500 °C for 2 h. We then returned the substrate back to the vacuum chamber and rotated the sample stage by 180°. Next, the Cu layer was deposited also at an oblique angle, forming roughly a chevron shape. After, the sample was annealed for a second time at 100 °C for 30 min, thus completing the desired TiO_2/Cu_2O hybrid structures. Each of the three samples were detached from the surface and suspended in pure water using bath sonication; examples are shown in the scanning electron microscopy (SEM, Zeiss Supra 40VP) images on the right side of Figure 1. Also shown in Figure 1 are elemental maps created by energy-dispersive X-ray spectroscopy (EDS, Thermo Scientific), which demarcate the location of the primary elements in each sample, labeled by the overlaid text.

Colloidal dispersions of the photoactive microswimmers were mixed with hydrogen peroxide and were given sufficient time ($\approx$1 min) to settle to the surface of a precleaned glass microscope slide. Although the full mechanism of self-propelled motion by means of a catalyzed chemical reaction is still not entirely understood, it is generally accepted that the breakdown of the chemical leads to the development of local concentration gradients, which in turn cause the particles to undergo autophoretic mobility at a speed $v \propto \nabla c$, where c is the concentration field.[47] In our system, photocatalysis of hydrogen peroxide on the semiconducting surfaces led to self-propulsion when light of sufficient energy was present, which is determined by the band gap of the material: $\approx$3.2 eV for anatase TiO_2 and $\approx$2.1 eV for Cu_2O. The decomposition of hydrogen peroxide $2H_2O_2 \rightarrow 2H_2O + O_2$ at the catalyst sites is expected to proceed by two different possible routes

$$H_2O_2 + 2e^- + 2H^+ \rightarrow 2H_2O$$
$$H_2O_2 + 2h^+ \rightarrow O_2 + 2H^+$$

(1)
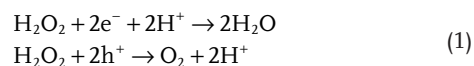
where e^- and h^+, are the electrons and holes generated, as pairs. In such systems, the strength of propulsion has been shown to be a function of the intensity of the activating light,[48] presumably by increasing the density of electron-hole pairs, and in some cases the concentration of hydrogen peroxide.[37] In the present study, we held the concentration of hydrogen peroxide constant at 1.5%(v/v) and we only changed the wavelength of the activating light. We first discuss the dynamics
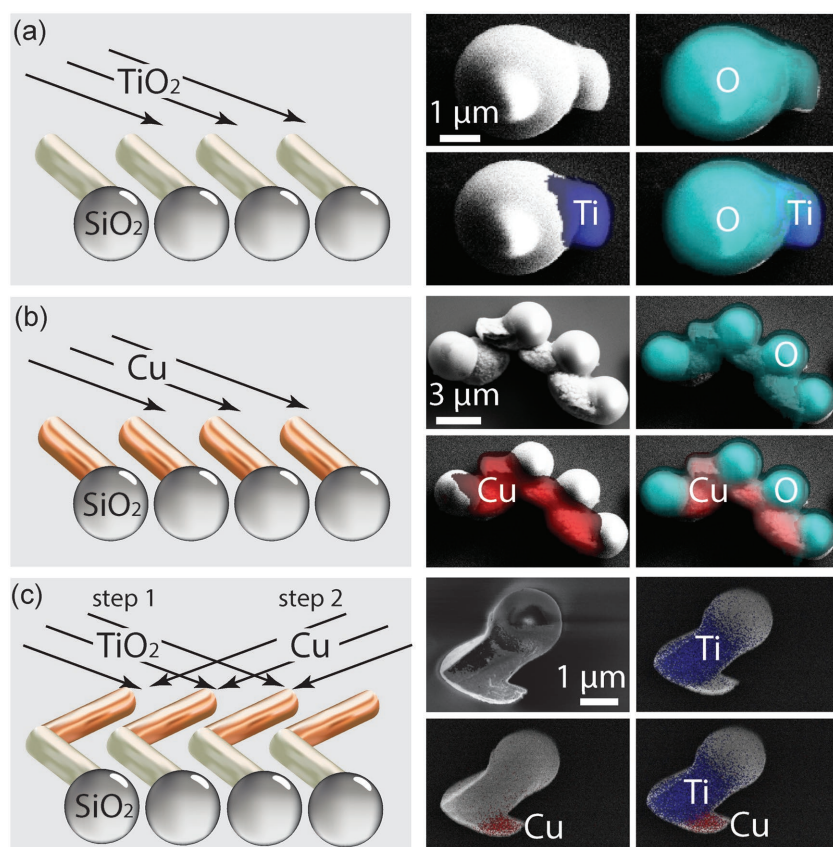

Figure 1. On the left side, schematics are shown depicting the fabrication of the three samples investigated in this study: a) TiO_2-only, b) Cu_2O-only, and c) hybrid TiO_2/Cu_2O microswimmers. Note that pure Cu is deposited in (b) and (c), which is converted to Cu_2O by annealing after deposition. On the right side, example SEM images with corresponding EDS spectroscopy-based elemental maps for each sample are shown.

of the single-photocatalyst microswimmers before turning our attention to the hybrid structures, in order to independently investigate the behavior of particles made from each individual material (TiO_2 or Cu_2O) alone.

When activated, the single-material microswimmers were propelled either toward or away from the oxide arms (see Videos S5 and S6 in the Supporting Information). We recently discovered the direction of motion is a function of such a particle's dimensions, and we discussed a possible propulsion mechanism for this system that we suspect is a combination of self-phoresis and osmotic flow over the stationary surface over which the particles move.[33] We note that the TiO_2 particles are highly impervious to degradation as expected for this material. However, Cu_2O becomes self-reduced over time to CuO, but our swimmers made from copper oxide remained active for several days before noticeable changes in the strength of propulsion arose. When exposed to hydrogen peroxide, the Cu_2O motors lost their activity over an even shorter period of time that was nevertheless longer than the timescale of the experiments. We inferred the strength of propulsion by determining the mean-squared displacement (MSD), as is appropriate for many self-propelled systems in the presence of significant noise. The MSD was calculated using the equation $\Delta r^2 = \langle [\vec{r}(t+\tau) - \vec{r}(t)]^2 \rangle$, where $\vec{r}$ is the 2D position of a particle and τ is the lag time. The curves in each plot of **Figure 2**a,b show the averaged MSD for at least 10 particles when exposed to one of the three colors of activating light supplied by a Zeiss AxioScope.A1 fluorescence microscope (UV (365 nm), blue (488 nm), and green (530 nm))—see the Supporting Information for spectra) for TiO_2-only and Cu_2O-only microswimmers, respectively. We measured the intensity of light at each wavelength and found that for UV and blue, the intensity was comparable ≈ 600 mW cm^{-2}, while the green light was only about one-fifth the strength of the other two colors ≈ 120 mW cm^{-2}. As can be seen in Figure 2a, the TiO_2-only particles are solely activated under UV-light, as expected, since a band gap of ≈ 3.2 eV corresponds to a wavelength of $\lambda \approx 390$ nm, while undergoing only Brownian motion in the presence of blue and green light, as indicated by the linear curves in Figure 2a. As Cu_2O has a band gap in the visible range ($\lambda \approx 590$ nm), particles made from this material are actively propelled when exposed to either UV or visible light, as can be inferred by the nonlinear curves of Figure 2b.

From these data, it appears the Cu_2O swimmers are slightly more active under blue light than UV, while being only weakly propelled in green light. As light intensity has been shown to affect the strength of propulsion,[48] the weak propulsion under green light is likely to stem from the significantly lower intensity at this wavelength.

We also deposited, and subsequently annealed, TiO_2 and Cu_2O semiconductor nanostructures grown directly onto quartz glass at an oblique angle of 85° and a nominal thickness of 100 nm in order to obtain ultraviolet–visible (UV–vis) spectra, which are shown in Figure 2c; the three peak excitation wavelengths are also indicated by the vertical lines on the graph. The thicknesses used to fabricate the microswimmers rendered the samples opaque, which is why the spectra are for hybrid nanoscale structures. Since we are only interested in the general trends of the optical absorbance, we expect the difference in size to have no significant qualitative effects upon the spectra. We also note that the spectra in Figure 2 are actually a measure of the extinction, i.e., combined absorbance and reflection, and not absorbance alone. Since the trends in the spectra are at least qualitatively similar to those in the literature that measure absorbance alone via diffuse reflectance spectroscopy,[49] we expect the main features of our spectra to arise from absorbance. TiO_2 absorbs primarily in the UV range (black curve) for $\lambda \lesssim 390$ nm, which is consistent with the MSD data shown in Figure 2a that indicate the TiO_2-only swimmers are activated by UV alone. Cu_2O absorbs visible wavelengths (red curve) with marked absorbance for $\lambda \lesssim 550$ nm, which is also consistent with the observed visible light activation of the Cu_2O-only microswimmers (Figure 2b). As the green light source is of higher energy (≈ 2.3 eV) than the band gap of Cu_2O (≈ 2.1 eV), we expected this source to lead to propulsion. However, as noted previously, the Cu_2O-only swimmers were only weakly propelled in green light, as shown in Figure 2b, which, as also stated previously, is likely due to the lower intensity at this wavelength. We note that the relatively low absorbance at $\lambda = 530$ nm in comparison to the other activating wavelengths is also consistent with this result. However, the magnitude of extinction does not necessarily translate directly to the strength of propulsion, as indicated by the significant difference between extinction at $\lambda = 488$ and 365 nm for Cu_2O (red curve in Figure 2c), despite
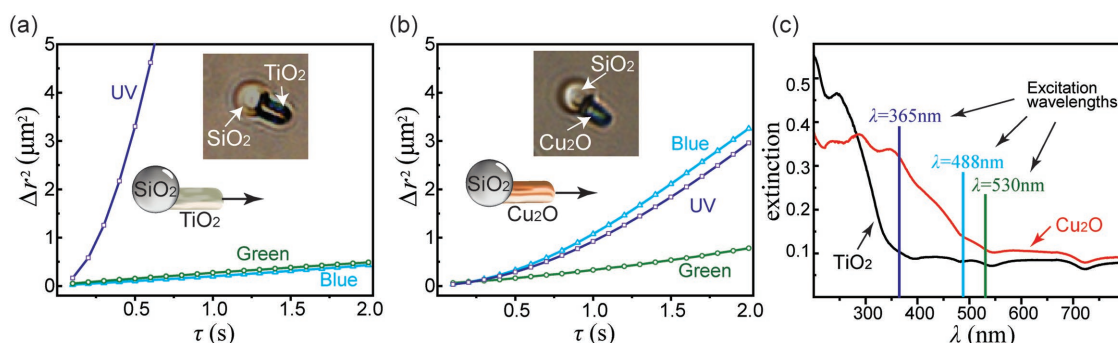
Figure 2. MSD curves for a) TiO_2- or b) Cu_2O-based microswimmers actuated under three different colors of light. The insets show micrographs of each particle type, and the overlaid text indicates the location of the materials from which the particles are made. c) UV–vis optical extinction spectra for nanostructures of TiO_2 (black curve) and Cu_2O (red curve) grown onto quartz glass at an oblique angle. The wavelengths of the three excitation sources are indicated by colored vertical lines as well.

the strength of propulsion being roughly the same (blue and purple curves in Figure 2b). Nevertheless, the important point is that the Cu_2O absorbs some visible wavelengths, while TiO_2 is active in the UV, as desired.

After developing an empirical basis for the behavior of swimmers made from each individual material, we next turn to the hybrid microswimmer made from both TiO_2 and Cu_2O. In order to demonstrate the different modes of motion clearly, the morphology we chose is approximately the shape of a chevron with each arm made from a different material: the arm adjacent to the microsphere is TiO_2 and the other is Cu_2O. An optical micrograph of a single hybrid particle is shown in **Figure 3**a, and the overlaid text indicates the location of the three different oxides, corroborated by the SEM data in Figure 1c. The optical extinction spectrum of an array of TiO_2/Cu_2O nanostructures on a transparent substrate is shown in Figure 3b as the black curve, while the red curve represents the (mathematical) addition of the spectra for each material given in Figure 2c. These spectra indicate the presence of both materials in the hybrid structure. Since we did not observe significant propulsion for either of the single material swimmers under green light (Figure 2a,b)—or for the hybrid structures—we chose instead another color that falls in between UV and blue: a violet laser diode (supplied by a Leica Confocal laser scanning microscope) with a peak wavelength of 405 nm. In Figure 3b, we have indicated the three wavelengths used to activate the hybrid swimmers as vertical lines: 365, 405, and 488 nm.

As Cu_2O is activated when exposed to any of these three colors, the hybrid microswimmers, which are partially made from this material, showed some form of activity at each wavelength. However, we did in fact find the mode of motion depends upon the activating light source, as desired. We note that increasing the intensity of the light at any tested wavelength caused the swimmers to rotate or translate at a higher rate. However, the mode of motion was not altered by changes in intensity. The oblique angle view in Figure 3c portrays the particles, which are held just above the solid surface of the observation cell by gravity, $\vec{g}$, moving either rotationally or translationally. As represented schematically in Figure 3c, translation is only observed for two wavelengths, $\lambda = 365$ and 405 nm (see Videos S1 and S2 in the Supporting Information) while rotation was observed for all three sources and presumably for the entire range $\lambda = 365$ to 488 nm (see Videos S3 and S4 in the Supporting Information). Since TiO_2 is only activated by UV, and because we only observe translational motion in this range, we suspect that the translational mode of motion, at speeds comparable to other systems of light-activated particles[40] ranging from ≈5 to 15 µm s^{-1}, results from the response of this portion of the particle (the 405 nm (peak) wavelength is likely to contain enough UV also to activate the TiO_2 portion). By extension, we suspect rotation results primarily from the activation of the Cu_2O arm. From these results, we find that for sufficiently long wavelength, only rotational motion will be present. Ideally, we would be able to actuate translational motion only toward the higher energy end of the spectrum, but both TiO_2 and Cu_2O are active in the UV range, and so we observe both rotation and translation for shorter wavelengths.

Although the two modes of motion cannot be decoupled in the UV, we found that the observed mode of motion appears to be strongly dependent upon a particle's orientation with respect
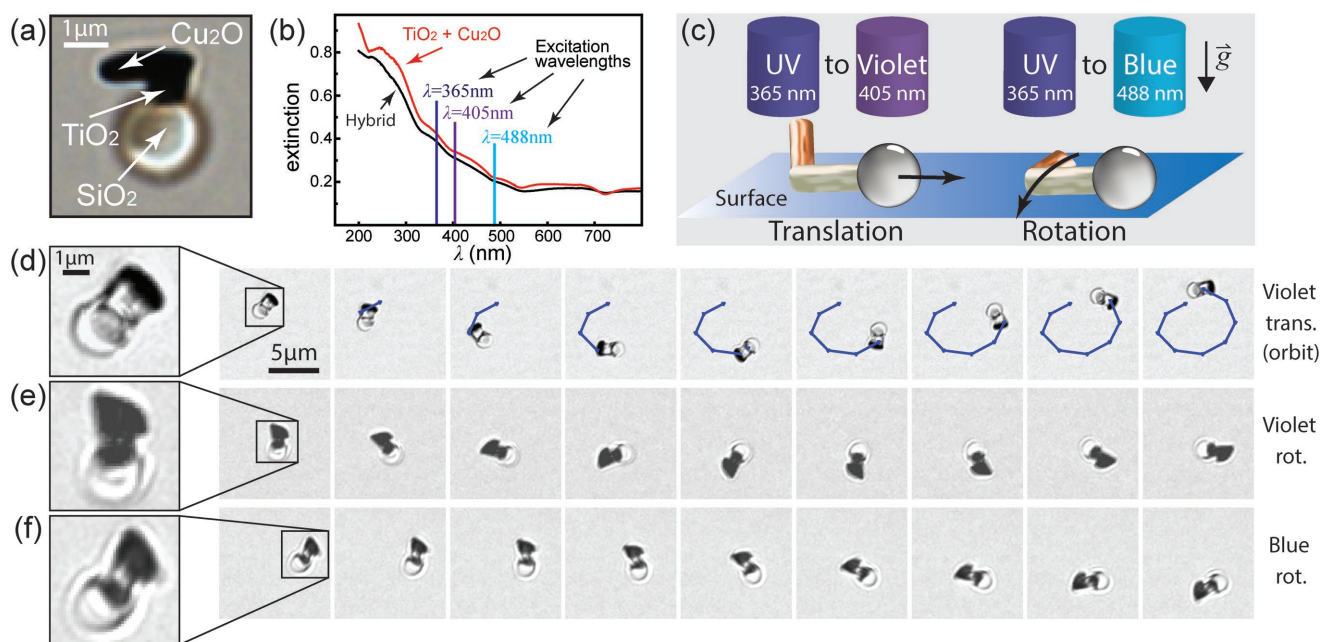
Figure 3. a) A high-resolution micrograph of a single hybrid microswimmer with labels showing the location of each material. b) The black curve shows UV–vis optical extinction spectra for the hybrid structures grown onto quartz glass, while the red curve results from the addition of the two spectra for the single photocatalysts. The excitation wavelengths are shown as vertical lines. c) Oblique angle schematic, with the direction of gravity indicated by $\vec{g}$, showing motive behavior over the solid surface as a function of the particle's orientation along with the activating light's color. d) Series of video frames separated by ≈0.1 s showing motive behavior in violet light for a single hybrid microswimmer when the Cu_2O tail is oriented out of the plane (left side of (c)). e) Rotational motion under violet light and f) rotational motion under blue light when the structures as situated "flat" against the surface.

to the plane over which it moves. If the Cu_2O tail is oriented out of the plane, the particle undergoes translational motion toward the SiO_2 head as shown schematically in Figure 3c. We note that the TiO_2-only swimmer in Video S5 of the Supporting Information moves toward the SiO_2 head, and the hybrid particles moved in this manner as well when moving translationally. The example video frames in Figure 3d (see Video S2 in the Supporting Information) demonstrate this effect—we chose a particle moving translationally in an orbital path for convenient illustration purposes. Video S1 shows a more typical translational motion that is approximately linear. See the Supporting Information for additional motion analysis for the different modes of motion. The Cu_2O arm is inferred to be oriented out of the plane by noting that only the TiO_2 arm, which is adjacent to the SiO_2 sphere, can be clearly resolved. On the contrary, both arms in the video frames in Figure 3e,f are apparent (see Videos S3 and S4 in the Supporting Information), suggesting the particle is positioned "flat" against the surface (right side of Figure 3c), and when oriented this way, the swimmers move in a rotational fashion. The video frames in Figure 3e,f show such rotational motion when the particles are exposed to violet or blue light, respectively. To reiterate, no translational motion was observed for the $\lambda = 488$ nm source regardless of orientation and so we may choose rotational motion alone by exposing the particles to blue light. On the other hand, for the $\lambda = 365$ or 405 nm sources, we obtain a mixed population of particles undergoing both translation and rotation. We suggest a means for inducing all particles in the population to undergo only one mode of motion: Since particle orientation determines whether rotational or translational motion occurs in the UV to violet range, by adding a small segment of a ferromagnetic material to the end of the Cu_2O arm, the application of an external magnetic field either in- or out-of-plane should lead to rotational and translational motion, respectively.

We note one other interesting observation about the hybrid microswimmer: The single semiconductor particles were not activated when exposed to any color of light if they were not also suspended in hydrogen peroxide. However, the hybrid structure was propelled under UV or violet light in H_2O alone. In **Figure 4**, we have classified the necessary

conditions—the chemical environment and color of activating light—for observing propulsion in all three samples investigated in this study. The shades of gray in the boxes indicate the chemical environment: the darkest shade for propulsion in either H_2O-alone or with hydrogen peroxide, the lighter shade for propulsion only when hydrogen peroxide is also present, and white for no motion with or without hydrogen peroxide. Although the hybrid structure was active without hydrogen peroxide (top two boxes in column 3), it should be noted that the activity was unambiguously increased when this chemical was added to the H_2O (we have not quantified this result here). A possible explanation for the hybrid swimmers being propelled in H_2O-alone is that a p–n semiconductor heterojunction (p-type Cu_2O and n-type TiO_2) has formed between the two materials,[49] which is known to suppress electron–hole recombination and consequently higher efficiency photocatalysis. As a type II heterojunction in which the valence and conduction bands are both higher in Cu_2O compared with TiO_2, we expect efficient charge separation.[50] We have provided an energy diagram for this heterojunction in the Supporting Information. In an analogous system, fuel free motion of TiO_2–gold Janus spheres was achieved facilitated by efficient charge separation at the metal–semiconductor Schottky junction.[36] We refer the reader to the Supporting Information for possible reaction pathways for the hybrid microswimmer in either water and hydrogen peroxide or water alone. We finally note that our system may be an attractive alternative to the oxide–metal swimmers as we are only using cheap and abundant semiconductors, as opposed to precious metals, and therefore the hybrid particles herein may prove to be the basis of a new class of fuel-free, all-semiconductor microswimmers.

In conclusion, we have developed a hybrid, multi-semiconductor photoactive microswimmer that undergoes wavelength-dependent motive behavior. The realization of such a morphology was made possible by employing a dynamic fabrication method that allows for constructing complex micro-structures from a wide range of materials and material combinations, which is ideal for this investigation. The hybrid micro-swimmers were made directly from two different photocatalysts, TiO_2 and Cu_2O, which catalyze hydrogen peroxide over differing ranges of wavelength. We believe all-semiconductor hybrid swimmers may not only be an effective means of actuating different modes of motion in a single particle, but may open up a new class of fuel-free swimmers without the need for precious metals. We have demonstrated a proof of concept in this Communication, but the method is not limited to the specific materials and geometries utilized herein. Future investigations will focus upon decoupling the different modes of motion, wavelength-dependent self-assembly and collective behavior of hybrid, semiconducting microswimmers, and the effects of semiconductor heterojunctions for fuel-free microscale photo-active matter.

	TiO₂	Cu₂O	Hybrid
UV	Trans.	Trans.	Trans./Rot.
Violet	Trans.	Trans.	Trans./Rot.
Blue	No motion	Trans.	Rot.
Green	No motion	Trans.	No motion

Key
H₂O only / H₂O₂+H₂O
H₂O₂+H₂O
No motion

Figure 4. Summary of the types of motion observed, either translation or rotation, for each microswimmer investigated in this study when exposed to the four wavelengths of activating light. The key on the right side indicates the chemical environment: the darker shade means motion in H_2O-alone or with hydrogen peroxide, the lighter shade indicates hydrogen peroxide is necessary to observe motion, and white is reserved for no motion being observed regardless of the chemical environment.

Supporting Information

Supporting Information is available from the Wiley Online Library or from the author.

[1] J. Elgeti, R. G. Winkler, G. Gompper, *Rep. Prog. Phys.* **2015**, *78*, 056601.

[2] I. S. Aranson, *Phys. Usp.* **2013**, *56*, 79.

[3] S. Ebbens, *Curr. Opin. Colloid Interface Sci.* **2016**, *21*, 14.

[4] H. Yu, A. Kopach, V. R. Misko, A. A. Vasylenko, D. Makarov, F. Marchesoni, F. Nori, L. Baraban, G. Cuniberti, *Small* **2016**, *12*, 5882.

[5] Y. Tu, F. Peng, D. A. Wilson, *Adv. Mater.* **2017**, *29*, 1701970.

[6] R. J. Archer, A. J. Parnell, A. I. Campbell, J. R. Howse, S. J. Ebbens, *Adv. Sci.* **2018**, *5*, 1700528.

[7] J. Palacci, S. Sacanna, A. P. Steinberg, D. J. Pine, P. M. Chaikin, *Science* **2013**, *339*, 936.

[8] A. Nourhani, S. J. Ebbens, J. G. Gibbs, P. E. Lammert, *Phys. Rev. E* **2016**, *94*, 030601.

[9] U. Choudhury, A. V. Straube, P. Fischer, J. G. Gibbs, F. Höfling, *New J. Phys.* **2017**, *19*, 125010.

[10] M. E. Cates, J. Tailleur, *Annu. Rev. Condens. Matter Phys.* **2015**, *6*, 219.

[11] A. Nourhani, D. Brown, N. Pletzer, J. G. Gibbs, *Adv. Mater.* **2017**, *29*, 1703910.

[12] A. Zöttl, H. Stark, *J. Phys. Condens. Matter* **2016**, *28*, 253001.

[13] J. N. Johnson, A. Nourhani, R. Peralta, C. McDonald, B. Thiesing, C. J. Mann, P. E. Lammert, J. G. Gibbs, *Phys. Rev. E* **2017**, *95*, 042609.

[14] M.-J. Huang, J. Schofield, R. Kapral, *New J. Phys.* **2017**, *19*, 125003.

[15] L. Soler, S. Sánchez, *Nanoscale* **2014**, *6*, 7175.

[16] M. Safdar, S. U. Khan, J. Jänis, *Adv. Mater.* **2018**, *30*, 1703660.

[17] J. Wang, W. Gao, *ACS Nano* **2012**, *6*, 5745.

[18] B. Jurado-Sánchez, S. Sattayasamitsathit, W. Gao, L. Santos, Y. Fedorak, V. V. Singh, J. Orozco, M. Galarnyk, J. Wang, *Small* **2015**, *11*, 499.

[19] T. Mirkovic, N. S. Zacharia, G. D. Scholes, G. A. Ozin, *Small* **2010**, *6*, 159.

[20] L. F. Valadares, Y.-G. Tao, N. S. Zacharia, V. Kitaev, F. Galembeck, R. Kapral, G. A. Ozin, *Small* **2010**, *6*, 565.

[21] X. Ma, J. Katuri, Y. Zeng, Y. Zhao, S. Sanchez, *Small* **2015**, *11*, 5023.

[22] A. Nourhani, P. E. Lammert, *Phys. Rev. Lett.* **2016**, *116*, 178302.

[23] J. G. Gibbs, Y.-P. Zhao, *Small* **2009**, *5*, 2304.

[24] J. G. Gibbs, P. Fischer, *Chem. Commun.* **2015**, *51*, 4192.

[25] S. Michelin, E. Lauga, *Sci. Rep.* **2017**, *7*, 42264.

[26] T.-C. Lee, M. Alarcón-Correa, C. Miksch, K. Hahn, J. G. Gibbs, P. Fischer, *Nano Lett.* **2014**, *14*, 2407.

[27] W. F. Paxton, K. C. Kistler, C. C. Olmeda, A. Sen, S. K. St. Angelo, Y. Cao, T. E. Mallouk, P. E. Lammert, V. H. Crespi, *J. Am. Chem. Soc.* **2004**, *126*, 13424.

[28] W. Wang, W. Duan, A. Sen, T. E. Mallouk, *Proc. Natl. Acad. Sci. USA* **2013**, *110*, 17744.

[29] J. Zheng, B. Dai, J. Wang, Z. Xiong, Y. Yang, J. Liu, X. Zhan, Z. Wan, J. Tang, *Nat. Commun.* **2017**, *8*, 1438.

[30] K. Robbie, M. Brett, *J. Vac. Sci. Technol.* **1997**, *15*, 1460.

[31] A. G. Mark, J. G. Gibbs, T.-C. Lee, P. Fischer, *Nat. Mater.* **2013**, *12*, 802.

[32] H.-H. Jeong, A. G. Mark, J. G. Gibbs, T. Reindl, U. Waizmann, J. Weis, P. Fischer, *Nanotechnology* **2014**, *25*, 235302.

[33] D. Nicholls, A. DeVerse, R. Esplin, J. Castañeda, Y. Loyd, R. Nair, R. Voinescu, C. Zhou, W. Wang, J. G. Gibbs, *ACS Appl. Mater. Interfaces* **2018**, *10*, 18050.

[34] M. Ibele, T. E. Mallouk, A. Sen, *Angew. Chem., Int. Ed.* **2009**, *48*, 3308.

[35] M. Enachi, M. Guix, V. Postolache, V. Ciobanu, V. M. Fomin, O. G. Schmidt, I. Tiginyanu, *Small* **2016**, *12*, 5497.

[36] R. Dong, Q. Zhang, W. Gao, A. Pei, B. Ren, *ACS Nano* **2015**, *10*, 839.

[37] B. Jang, A. Hong, H. E. Kang, C. Alcantara, S. Charreyron, F. Mushtaq, E. Pellicer, R. Büchel, J. Sort, S. S. Lee, B. J. Nelson, S. Pané, *ACS Nano* **2017**, *11*, 6146.

[38] J. Palacci, S. Sacanna, A. Vatchinsky, P. M. Chaikin, D. J. Pine, *J. Am. Chem. Soc.* **2013**, *135*, 15978.

[39] D. P. Singh, W. E. Uspal, M. N. Popescu, L. G. Wilson, P. Fischer, *Adv. Funct. Mater.* **2018**, *28*, 1706660.

[40] D. Zhou, Y. C. Li, P. Xu, N. S. McCool, L. Li, W. Wang, T. E. Mallouk, *Nanoscale* **2016**, *9*, 75.

[41] J. Wang, Z. Xiong, X. Zhan, B. Dai, J. Zheng, J. Liu, J. Tang, *Adv. Mater.* **2017**, *29*, 1701451.

[42] F. Martinez-Pedrero, H. Massana-Cid, P. Tierno, *Small* **2017**, *13*, 1603449.

[43] R. Dong, Y. Hu, Y. Wu, W. Gao, B. Ren, Q. Wang, Y. Cai, *J. Am. Chem. Soc.* **2017**, *139*, 1722.

[44] C. Chen, S. Tang, H. Teymourian, E. Karshalev, F. Zhang, J. Li, F. Mou, Y. Liang, J. Guan, J. Wang, *Angew. Chem., Int. Ed.* **2018**, https://doi.org/10.1002/ange.201803457.

[45] P. Basnet, Y. Zhao, *Catal. Sci. Technol.* **2016**, *6*, 2228.

[46] D. Schamel, A. G. Mark, J. G. Gibbs, C. Miksch, K. I. Morozov, A. M. Leshansky, P. Fischer, *ACS Nano* **2014**, *8*, 8794.

[47] R. Golestanian, T. Liverpool, A. Ajdari, *New J. Phys.* **2007**, *9*, 126.

[48] D. P. Singh, U. Choudhury, P. Fischer, A. G. Mark, *Adv. Mater.* **2017**, *29*, 1701328.

[49] Y. Bessekhouad, D. Robert, J.-V. Weber, *Catal. Today* **2005**, *101*, 315.

[50] M. Janczarek, E. Kowalska, *Catalysts* **2017**, *7*, 317.